An Acad Bras Cienc (2024) 96(Suppl. 1): e20230382 DOI 10.1590/0001-3765202420230382
Anais da Academia Brasileira de Ciências | *Annals of the Brazilian Academy of Sciences*
Printed ISSN 0001-3765 I Online ISSN 1678-2690
www.scielo.br/aabc | www.fb.com/aabcjournal

CELLULAR AND MOLECULAR BIOLOGY

Expression and purification of active shikimate dehydrogenase from *Plasmodium falciparum*

BRUNO G. DALLA VECCHIA MORALES, JOSEPH ALBERT M. EVARISTO, GEORGE A.R. DE OLIVEIRA, ANA FIDELINA G. GARAY, JORGE JAVIER A.R. DIAZ, ANDRELISSE ARRUDA, SORAYA S. PEREIRA & FERNANDO B. ZANCHI

Abstract: *Plasmodium falciparum* is known to cause severe malaria, current treatment consists in artemisinin-based combination therapy, but resistance can lead to treatment failure. Knowledge concerning *P. falciparum* essential proteins can be used for searching new antimalarials, among these a potential candidate is shikimate dehydrogenase (SDH), an enzyme part of the shikimate pathway which is responsible for producing endogenous aromatic amino acids. SDH from *P. falciparum* (P*f*SDH) is unexplored by the scientific community, therefore, this study aims to establish the first protocol for active P*f*SDH expression. Putative P*f*SDH nucleotide sequence was used to construct an optimized expression vector pET28a+P*f*SDH inserted in *E. coli* BL21(DE3). As a result, optimal expression conditions were acquired by varying IPTG and temperature through time. Western Blot analysis was applied to verify appropriate P*f*SDH expression, solubilization and purification started with lysis followed by two-steps IMAC purification. Enzyme activity was measured spectrophotometrically by NADPH oxidation, optimal P*f*SDH expression occur at 0.1 mM IPTG for 48 hours growing at 37 °C and shaking at 200 rpm, recombinant P*f*SDH obtained after purification was soluble, pure and its physiological catalysis was confirmed. Thus, this study describes the first protocol for heterologous expression of P*f*SDH in soluble and active form.

Key words: Active enzyme, malaria, *P. falciparum*, protein expression, protein purification, shikimate dehydrogenase

INTRODUCTION

Plasmodium falciparum is the protozoan known to cause severe malaria; a globally endemic disease responsible for 247 million cases and 619,000 deaths worldwide, most of these occurring in Africa, where *P. falciparum* is the prevalent etiological agent (World Health Organization 2022). *P. falciparum* displays certain virulence factors that distinguish it from the other species of *Plasmodium* spp. that are capable of infecting humans, such as the secretion of the ring-infected surface antigen 1 (RESA1) (Bozdech et al. 2003), the alteration of the coagulation cascade, a high parasitemia during erythrocyte phase (Bougard et al. 2018) and the induction of cytoadherence of erythrocytes to the walls of the blood vessel (Dondorp et al. 2004).

Since the evolution to the severe form of the disease affects the central nervous system, causes acute renal failure, severe anemia and acute respiratory distress syndrome (ARDS), treatment is recommended within 24 hours of the onset of symptoms (Centers for Disease Control and Prevention 2019). Current treatment for *P. falciparum* infection consists of an artemisinin-based combination therapy (ACT), in which artemisinin is combined with a drug from a different class. This approach is essential in

order to prevent *P. falciparum* from presenting resistance to the mode of action of a particular drug, consequently rendering an entire family of drugs ineffective. Resistance to antimalarials by *P. falciparum* can be defined as: I: partial resistance to artemisinin; II: multidrug resistance, when two or more drugs are ineffective (a characteristic associated with chloroquine and pyrimethamine-sulfadoxine resistant *P. falciparum* infections); and III: treatment failure, when no drug is able to stop the growth of the parasite; these are factors that lead to the search for a greater number of alternative therapies (Fairhurst & Dondorp 2016).

The construction of genome, metabolome and proteome libraries based on the incorporation of molecular and computational strategies paves the way for the search for new antimalarial therapies based on rationally designed and experimentally validated processes, which are especially focused on identifying and exploring key parasitic processes (Ferreira et al. 2018). Therefore, the knowledge of proteins that play fundamental roles in the maintenance and continuity of essential biochemical pathways of *P. falciparum* is decisive in determining a molecular target that can be used as a basis for the search for new antimalarials that are designed in a completely rational way (Kumar et al. 2018).

Among the various targets, shikimate dehydrogenase (SDH) (EC 1.1.1.25), an oxidoreductase part of the shikimate pathway with a molecular mass of approximately 22 kDa, stands out. It is the fourth enzyme in this pathway and is responsible for catalyzing the reversible chemical reaction 3-dehydroshikimate (DHS) + NADPH ⇌ Shikimate (SHK) + NADP+ (Figure 1). It is composed of an N-terminal substrate-binding domain and a C-terminal cofactor-binding domain (Díaz-Quiroz et al. 2018). The shikimate pathway is mainly responsible for producing endogenous aromatic amino acids (Díaz-Quiroz et al. 2018) and is present in plants, bacteria, fungi and Apicomplexa protozoa, though absent in vertebrates (Sutton et al. 2016). Furthermore, the pathway's final product is chorismate, a metabolite necessary for the endogenous synthesis of many molecules, such as the aromatic amino acids phenylalanine, tryptophan and tyrosine. Among these molecules is pABA

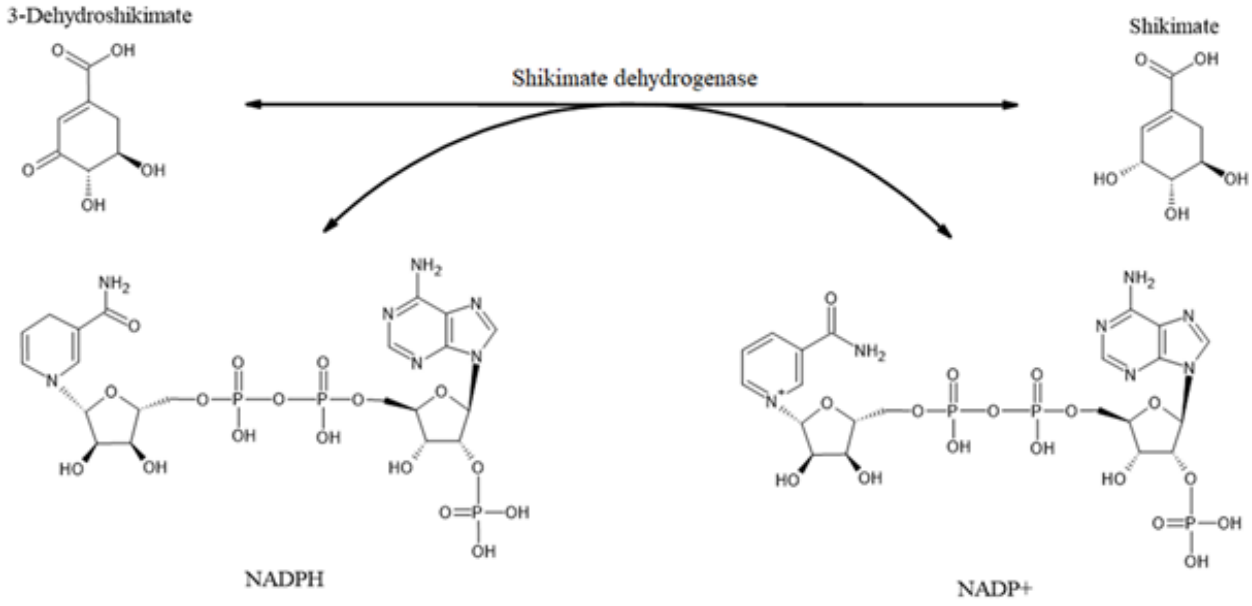

Figure 1. Enzyme reaction catalyzed by shikimate dehydrogenase (SDH).

(4-aminobenzoate), a substrate of folate, an obligatory endogenously synthesized molecule in the Apicomplexa parasite *P. falciparum* (McConkey 1999). Therefore, a direct inhibitory effect on enzymes of the shikimate pathway interferes, in the form of a cascade, on the production of endogenous folate.

Although SDH has been a target of functional and structural studies that have searched for inhibitors, it remains scarcely studied when compared to other enzymes of its pathway (Díaz-Quiroz et al. 2018). The role of SDH from *P. falciparum* as a potential target for drug discovery is still unexplored by the scientific community; therefore, this study aims to establish the first protocol for *in vitro* production of recombinant shikimate dehydrogenase from *Plasmodium falciparum* in soluble form using a prokaryotic system.

MATERIALS AND METHODS

Construction of expression vector and cDNA extraction

The putative nucleotide sequence of shikimate dehydrogenase from *Plasmodium falciparum* (P*f*SDH) was obtained from the GenBank database, code XM_001348562 (Gardner et al. 2002), and submitted to BLAST (Altschul et al. 1990) to identify similar sequences, followed by multiple sequence alignment using Clustal Omega (Sievers et al. 2011) to identify conserved regions. Sequence formatting was done using Jalview (Waterhouse et al. 2009). Synthesis of the expression vector was carried out by FastBio Ltda. (Ribeirão Preto, Brazil) in a vector harboring the coding gene optimized for expression in *Escherichia coli* and a hexa-histidine marker (His-tag) in the C-terminal region.

The expression vector was replicated by transformation into *E. coli* TG1 for DNA multiplication and extracted using a QIAprep Spin Miniprep kit (QIAGEN) according to the manufacturer's recommendations, followed by quantification using spectrophotometry (NanoDrop 2000, Thermo Fisher Scientific, Waltham, USA).

Expression of P*f*SDH under optimal induction circumstances

Transformation, induction and lysis steps were adapted from Sambrook & Russell (2001). For the transformation, 20 ng/µL of pET28a+P*f*SDH were inserted in electrocompetent *E. coli* BL21(DE3) and electroporated with a pulse of 1.6 kV for 4.7 ms. Immediately after electroporation, SOC (tryptone, yeast extract, NaCl, 20% glucose, 1 M $MgCl_2$ and 1 M $MgSO_4$) was added to the sample, followed by incubation for 1 hour at 37 °C and shaking at 200 rpm. After incubation, the culture was spread on a Petri dish containing LB agar supplemented with kanamycin (25 µg/mL), which was followed by another incubation at 37 °C overnight.

An isolated colony-forming unit was inoculated in liquid LB culture medium (v 1:50) supplemented with kanamycin (25 µg/mL) as a starter culture and incubated at 200 rpm and 37 °C overnight, which was followed by another incubation under the same conditions and was grown until it reached an optical density of 0.6 at a wavelength of 600 nm (OD_{600}). In order to determine the optimal duration of growth and concentration of transcription inducer IPTG (isopropyl β-D-1-thiogalactopyranoside) for expression, the culture was fractionated into four equal volumes. In three of these, IPTG was added to each at concentrations of 0.1 mM, 0.5 mM and 1.0 mM. As the control, the fourth fraction was grown without IPTG. The OD_{600} of all the cultures was measured at intervals from 1 to 8, 24, 48 and 72 hours. All the OD_{600} measurements were obtained via spectrophotometry (BioMate 3, Thermo Scientific, Waltham, USA). A temperature

of 37 °C and shaking at 200 rpm were standard for all cultures. Replicates were not employed. For the construction of the bacterial growth curve, the Prism 9.0.0 program (GraphPad Software, La Jolla California, USA) was used.

Western Blot analysis

In order to verify the expression of recombinant P*f*SDH after induction, the Western Blot technique, adapted from Hirano (2012), was performed and used anti-His-tag antibodies (Sigma-Aldrich). An aliquot of 10 µg of protein from cultures grown for 4, 24 and 48 hours was reduced using dithiothreitol (DTT) and applied to one-dimensional electrophoresis using 12% SDS-PAGE and transferred to a nitrocellulose membrane. Reactive sites were blocked with 5% skimmed milk in TBS buffer (TBSM) at 4 °C overnight. After blocking, the membrane was washed with TBS buffer + 0.1% Tween 20 (TBST) and incubated with the anti-His primary antibody (1:1000 in 5% TBSM) (GE Healthcare) at 4 °C overnight. After washing again with TBST, the membrane was incubated with the secondary anti-mouse IgG antibody produced in goat and conjugated to HRP (1:3,000 in 5% TBSM). Reactive signals were detected by incubation with hydrogen peroxide in DAB (diaminobenzidine) solution (SIGMAFAST DAB with Metal Enhancer, Sigma-Aldrich) for chemiluminescent detection. For the positive control, SDAg-III was used as a laboratory standard.

Solubilization and purification of recombinant P*f*SDH

The lysis, purification and protein concentration steps were adapted from Loughran et al. (2017). After defining the ideal expression conditions, the culture was centrifuged at 12,300 x *g* for 15 minutes at 4 °C. Cell precipitate was resuspended in lysis buffer (20 mM Tris, 500 mM NaCl, 10% glycerol at pH 8) plus 1% Triton X-100 (Vetec Química Fina LTDA.), with the volume equal to 10% of the induced culture volume. Throughout the lysis process, the resuspended cells were kept on ice. Cell lysis was performed using an ultrasonic probe (Q700 Sonicator, QSonica) at 40% amplitude for a total of 10 minutes, 30 seconds on and 45 seconds off. Sonication was repeated, if necessary, until no viscosity was observed. Finally, the bacterial lysate was centrifuged at 12,300 x *g* for 15 minutes at 4 °C for sedimentation of cell debris, and the supernatant was carried over for purification.

The recombinant P*f*SDH was purified via immobilized metal affinity chromatography (IMAC) using a column with nickel agarose resin (Ni-NTA Agarose, QIAGEN) (Petty 2001) coupled to a FPLC purification system (AKTA Purifier, GE Healthcare). The entire purification process was at a flow rate of 1 mL/min and was monitored at 280 nm. The column was equilibrated with equilibration buffer (50 mM Tris, 300 mM NaCl, 20 mM imidazole) using a volume equal to the volume of three columns. The lysate was loaded into the column with the aid of a peristaltic pump under the same conditions as those described above. After injection of the lysate, the equilibration buffer was applied to wash the non-specific bound proteins, followed by elution buffer (50 mM Tris, 300 mM NaCl, 250 mM imidazole) in a linear gradient of 15 minutes from zero to 100% for the elution of the recombinant protein.

Protein concentration was determined using a DC Protein Assay kit (Bio-Rad Laboratories) according to the manufacturer's recommendations and by using bovine serum albumin (BSA) as the standard. The theoretical molecular mass was obtained via the ExPASy ProtParam tool (Gasteiger et al. 2005) using the P*f*SDH amino acid sequence coupled to a six-histidine tag.

Both expression and purification were monitored using 15% polyacrylamide gel electrophoresis with the addition of sodium dodecyl sulfate (SDS-PAGE). Samples were prepared with 100 mM Tris-HCl, 4% SDS, 0.2% bromophenol blue, 20% glycerol, 1% DTT, pH 6.8 and denatured at 96 °C for 10 minutes (Laemmli 1970). After migration, the gels were stained with Coomassie blue and destained with 40% ethanol + 20% glacial acetic acid for visualization of the bands. The SDS-PAGE images were visualized using ImageJ 1.53c software (Schneider et al. 2012).

Analysis of enzyme activity

The enzyme activity assay was adapted from Díaz-Quiroz et al. (2018). The substrate 3-dehydroshikimate (DHS) (MilliporeSigma) and cofactor NADPH (Santa Cruz Biotechnology) were acquired from specialized companies. A linear physiological reaction was employed and P*f*SDH catalysis was monitored via NADPH oxidation absorbance over time at a wavelength of 340 nm and measured via spectrophotometry (PowerWave XS2, BioTek Instruments) at room temperature. The total analysis took one hour and twenty-five minutes.

The reaction was observed by adding 0.2 mM NADPH to 100 mM KH_2PO_4, 855 µg/mL P*f*SDH, 1.2 mM DHS, pH 7.5. The control sample was subjected to the same reaction solution, although without DHS (100 mM KH_2PO_4, 0.2 mM NADPH, 855 µg/mL P*f*SDH, pH 7.5). The final volumes of all samples were 200 µL, and triplicates were applied.

A graph was generated from the absorbance readings values (y axis) according to elapsed time (x axis) using Microsoft Excel 2019 (Microsoft, Seattle, USA) to acquire the equation of the trendline for each sample. From this equation, the consumption constant of NADPH per minute was obtained (Frutuoso, unpublished data). The graph shown was created using the Prism 9.0 program (GraphPad Software, La Jolla, USA).

RESULTS

Expression vector

The nucleotide sequence of shikimate dehydrogenase from *Plasmodium falciparum* (P*f*SDH) (XM_001348562) submitted to BLAST returned 21 similar sequences with a minimum query cover of 98%, an E-value of zero and a minimum percentage of identity of 92%. Only the sequences with 100% query cover were selected for examining the conserved regions. The sequences identified were XM_012910037 from *P. reichenowi* (Sundararaman et al. 2016), XM_018788134 from *P. gaboni* (Sundararaman et al. 2016) and XM_028684730 from *Plasmodium* sp. gorila clade G2 (National Center for Biotechnology Information 2019). Few divergences can be noticed between the nucleotides at the same position, with a total of 47 divergent positions (Figure 2). Among these divergences, 17 had only one nucleotide mutation (75% similarity) and 30 had two nucleotide mutations (50% similarity); no position showed more than two different nucleotides. This multiple alignment showed a similarity that was greater than 92% between all analyzed sequences (Table I). This result allows us to infer that the coding sequence gene of shikimate dehydrogenase from *Plasmodium* spp. is highly conserved.

Expression of P*f*SDH in *E. coli* BL21(DE3) and solubilization

Using the parameters analyzed during the determination of the ideal induction conditions, a bacterial growth curve was created, observing the variation in optical density via growth under induction (Figure 3). All samples reached a stationary phase within 48 hours. Bacterial death was observed in the control and in the

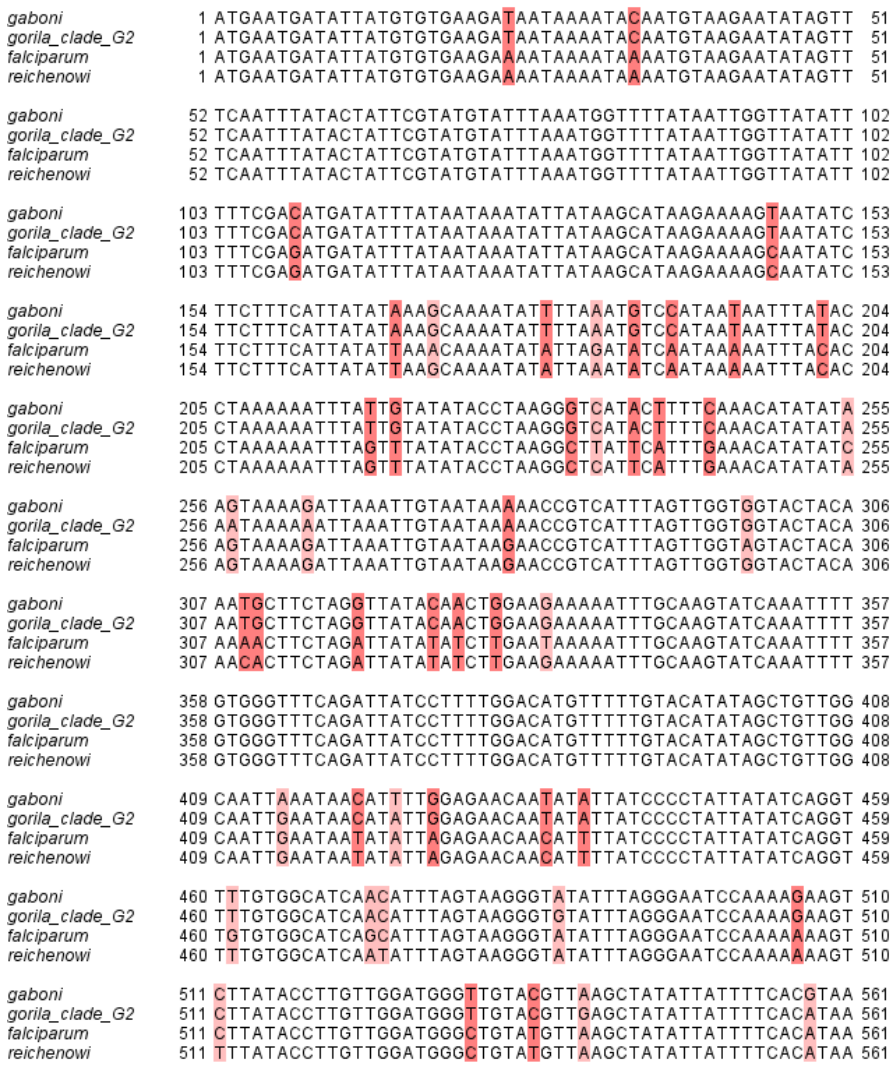

Figure 2. Multiple sequence alignment of shikimate dehydrogenase from *Plasmodium* spp. indicating the nucleotide divergence level in each position. Light red = one nucleotide divergence; dark red = two nucleotide divergences. Falciparum: *Plasmodium falciparum* (XM_001348562). Reichenowi: *Plasmodium reichenowi* (XM_012910037). Gaboni: *Plasmodium gaboni* (XM_018788134). Gorila clade G2: *Plasmodium sp.* gorila clade G2 (XM_028684730).

1.0 mM IPTG sample at 72 hours of growth in both. Both the 0.1 mM and 0.5 mM IPTG samples followed the same growth pattern and remained in the stationary phase for up to 72 hours.

To determine the ideal induction conditions, the presence or absence of bands consistent with the theoretical molecular mass (MW) of P*f*SDH were also considered, with addition of MW from the His-tag, defined at 22.7 kDa according to ExPASy ProtParam (Schneider et al. 2012), and visible using 15% SDS-PAGE in selected samples (Figure 4). P*f*SDH was successfully expressed under the analyzed circumstances, as can be seen by the presence of a band that is consistent with its theoretical MW of 22.7 kDa in all induced cultures regardless of the IPTG concentration. Absence of a marked band in this MW range in wells referring to uninduced culture evidences the requirement of IPTG for expression of P*f*SDH, which is characteristic of the expression of recombinant proteins using pET28a (Shilling et al. 2020).

In the analysis of the polyacrylamide gels referring to the testing of the ideal induction period (Figure 4a, b and c), the band referring to P*f*SDH is more noticeable at periods of 24, 48 and 72 hours. At 72 hours, there is evidence of a greater concentration of bacterial proteins;

Table I. Percentage of similarity between shikimate dehydrogenase sequences selected with 100% query cover.

Code	XM_001348562	XM_012910037	XM_018788134	XM_028684730
XM_001348562	-	98.04%	92.69%	92.51%
XM_012910037	98.04%	-	93.76%	93.58%
XM_018788134	92.69%	93.76%	-	98.75%
XM_028684730	92.51%	93.58%	98.75%	-

XM_001348562: *P. falciparum*; XM_012910037: *P. reichenowi*; XM_018788134: *P. gaboni*; XM_028684730: *Plasmodium sp.* gorila clade G2.

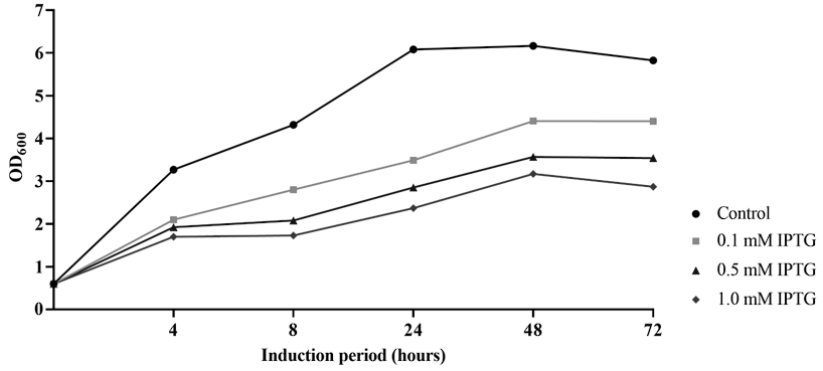

Figure 3. Bacterial growth curve of *E. coli* BL21(DE3)+pET28a(P*f*SDH) under varying concentrations of IPTG. Ratio of 600 nm optical density (OD_{600}) to induction time (hours) of three concentrations of IPTG (isopropyl β-d-1-thiogalactopyranoside) in *E. coli* BL21(DE3)+pET28a(P*f*SDH) cellular growth under recombinant P*f*SDH expression. Control has no IPTG. Periods of 1, 2, 3, 5, 6 and 7 hours are suppressed.

however, the P*f*SDH concentration shows no increase in intensity. There was no significant difference in expression between IPTG concentrations regarding the periods sampled.

Western Blot analysis

In order to confirm the presence of recombinant P*f*SDH after the expression process, Western Blot was applied. While the optimal IPTG concentration for induction is known to be 0.1 mM, induction periods of 4, 24, and 48 hours were also examined (Figure 5). Although it had been previously determined that the 48-hour time point was optimal, based on prior tests, samples from 4 and 24 hours were also included to assess whether there would be any discernible differences in band intensity during the experiment. Alongside the induced cells, cultures without induction for each period were also assessed. Notably, the signal presence was observed exclusively in the induced cells and was absent in the non-induced cells. Furthermore, the MW pattern was consistent with the theoretical MW of P*f*SDH+His-tag, indicating uniform protein expression across all the induction periods examined (Figure 5b).

IMAC purification of recombinant P*f*SDH

Purification of P*f*SDH obtained after expression was performed using immobilized metal affinity chromatography (IMAC) with a 5 mL column containing nickel resin (Ni-NTA Agarose). P*f*SDH was eluted with a gradient from 20 to 250 mM of imidazole obtaining 855 µg/mL of P*f*SDH measured using a DC Protein Assay kit. The chromatogram obtained via the FPLC AKTA Purifier system showed only one peak in the absorbance of 280 nm after the beginning of the imidazole gradient (Figure 6).

In the analysis of the eluate using SDS-PAGE 15%, it was possible to observe the effective migration of P*f*SDH according to its theoretical MW. A higher band, above the one referring to P*f*SDH in the eluate, is noticeable and, therefore, it is not possible to consider the sample as pure (Figure 6b).

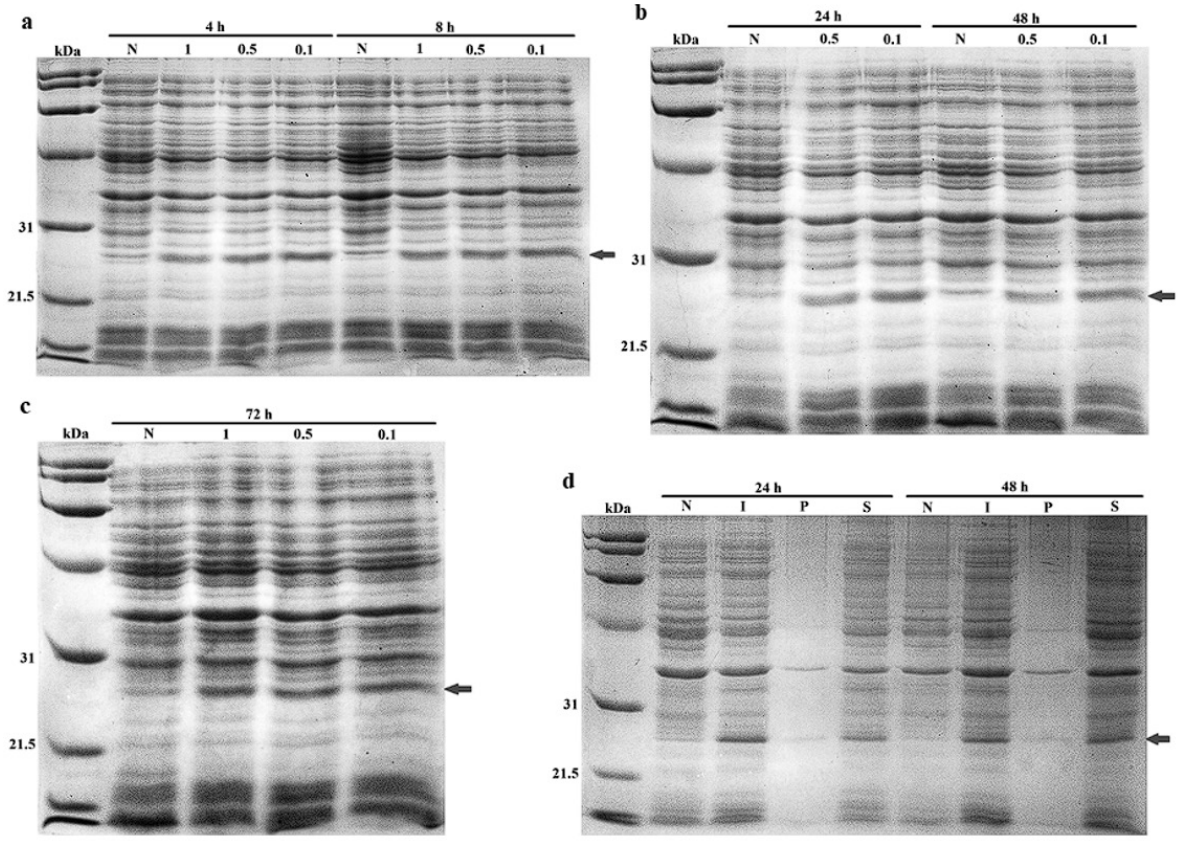

Figure 4. SDS-PAGE 15% Coomassie blue stained samples using the bacterial growth curve. Attempts to standardize the induction of P*f*SDH expression in *E. coli* BL21(DE3) at 37 °C. (a) Induction for 4 and 8 hours. N: not induced; 1: 1.0 mM IPTG; 0.5: 0.5 mM IPTG; 0.1: 0.1 mM IPTG. (b) induction for 24 and 48 hours. N: not induced; 0.5: 0.5 mM IPTG; 0.1: 0.1 mM IPTG. (c) Induction for 72 hours. N: not induced; 1: 1.0 mM IPTG; 0.5: 0.5 mM IPTG; 0.1: 0.1 mM IPTG. (d) Samples induced for 24 and 48 hours with 0.1 mM IPTG showing wells after lysis process. N: not induced; I: induced; P: pellet; S: soluble. Red arrow indicates migration of P*f*SDH according to theoretical MW containing His-tag.

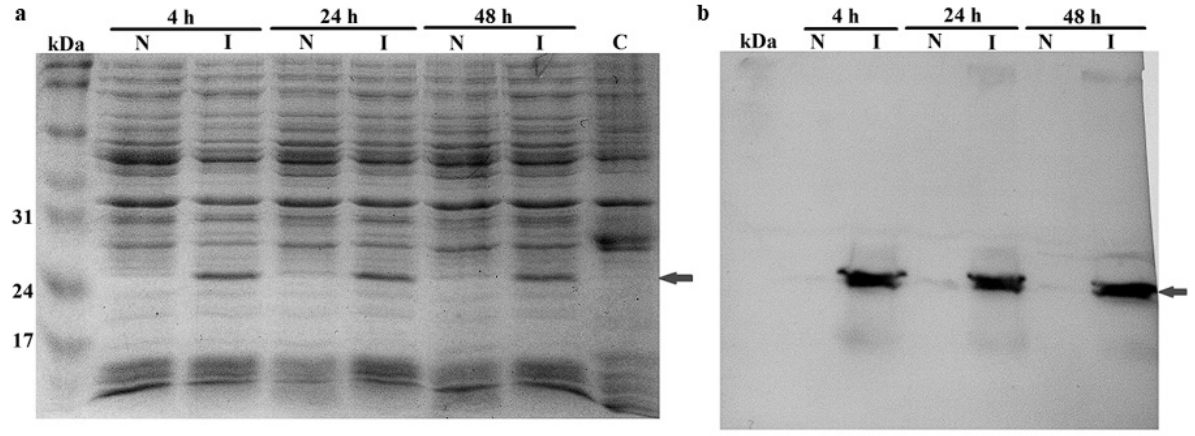

Figure 5. Western Blot after induction. (a) Mirror 15% SDS-PAGE after induction of bacterial culture. (b) Western blot reaction after electro transfer to nitrocellulose membrane and staining by hydrogen peroxide in diaminobenzidine (DAB) solution. 4 h, 24 h and 48 h: induction time by 0.1 mM IPTG at 37 °C and 200 rpm. N: not induced; I: induced; C: SDAg-III as a positive control. Red arrow indicates migration of P*f*SDH containing His6 tag according to theoretical MW.

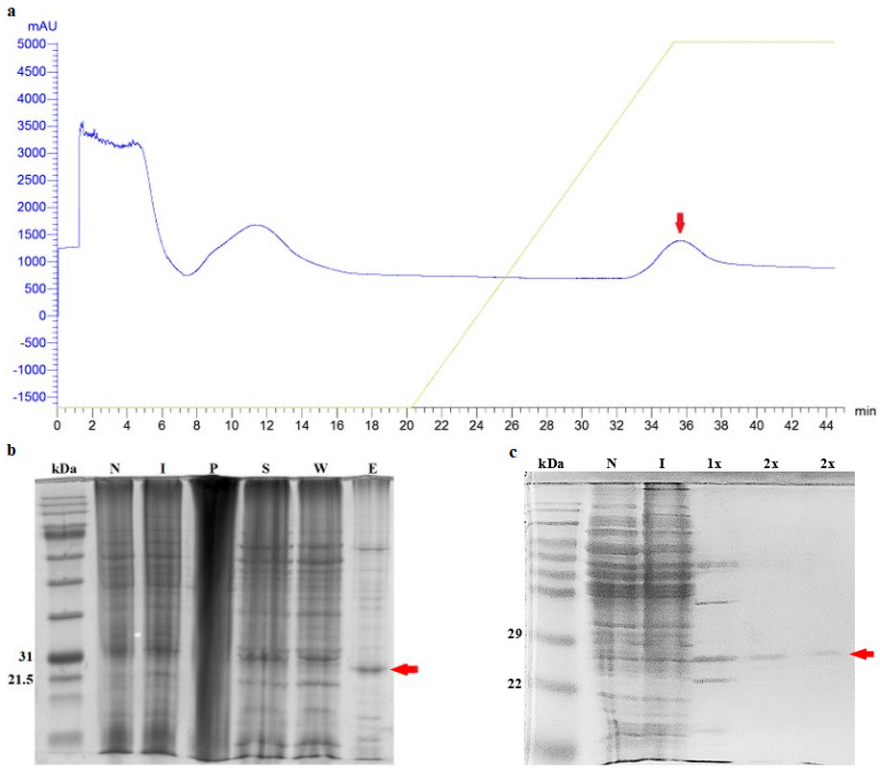

Figure 6. IMAC purification of P*f*SDH. (a) IMAC chromatogram with the elution profile after injection in the column containing nickel resin (Ni-NTA Agarose). P*f*SDH appears as a single peak after imidazole gradient 20 – 250 mM (0 – 100%) for 15 minutes. Red arrow indicates eluted P*f*SDH peak. Ab_{280} in blue. Gradient in green. (b) 15% SDS-PAGE of IMAC purified P*f*SDH. N: not induced, I: induced by 0.1 mM IPTG, P: lysate pellet, S: lysate supernatant, W: wash, E: eluate. (c) 15% SDS-PAGE of IMAC purified P*f*SDH. N: not induced, I: induced by 0.1 mM IPTG, 1x: one IMAC purification step, 2x: two IMAC purification steps. Red arrow indicates migration of P*f*SDH according to theoretical MW containing His-tag.

P*f*SDH physiological enzymatic activity

It is possible to observe the consumption of NADPH by the decrease of its concentration in the enzymatic reaction solution over the sampled period, suggesting SHK production in accordance with the linear enzymatic reaction of P*f*SDH (Figure 7). A slight downslope is also observed in the control sample, although NADPH consumption is < 0.001 mM. In this study, we chose to use the natural sense of the reaction since the *in vitro* experiment would have greater similarity with what happens *in vivo*, since the final objective of recombinant expression of this protein is to obtain it with its catalytic biological activity preserved (Structural Genomics Consortium et al. 2008). Knowing that NADPH absorbs UV light at a wavelength of 340 nm, its reduction was used to monitor the reaction and its concentration was set at 0.2 mM since it is a concentration usually found at a cellular level and due to it being sufficiently captured by spectrophotometry (Veskoukis et al. 2018).

DISCUSSION

Optical density had a significant oscillation between analyzed samples during the expression cell growth step and was predominantly higher in the non-induced control. Among the induced cultures, the lowest concentration of IPTG tested (0.1 mM) achieved the highest value (OD_{600} = 4.408), in contrast to the highest inductor concentration (1.0 mM). This behavior is observed in the literature, whereby a high concentration of IPTG leads to low cell growth, plasmid segregation and formation of inclusion bodies, as cellular machinery is applied to mRNA translation into recombinant P*f*SDH (Einsfeldt et al. 2011; Marí et al. 1999; Xu et al. 2006). It is important that the lowest possible concentration of the inductor is administered so that its toxicity may be

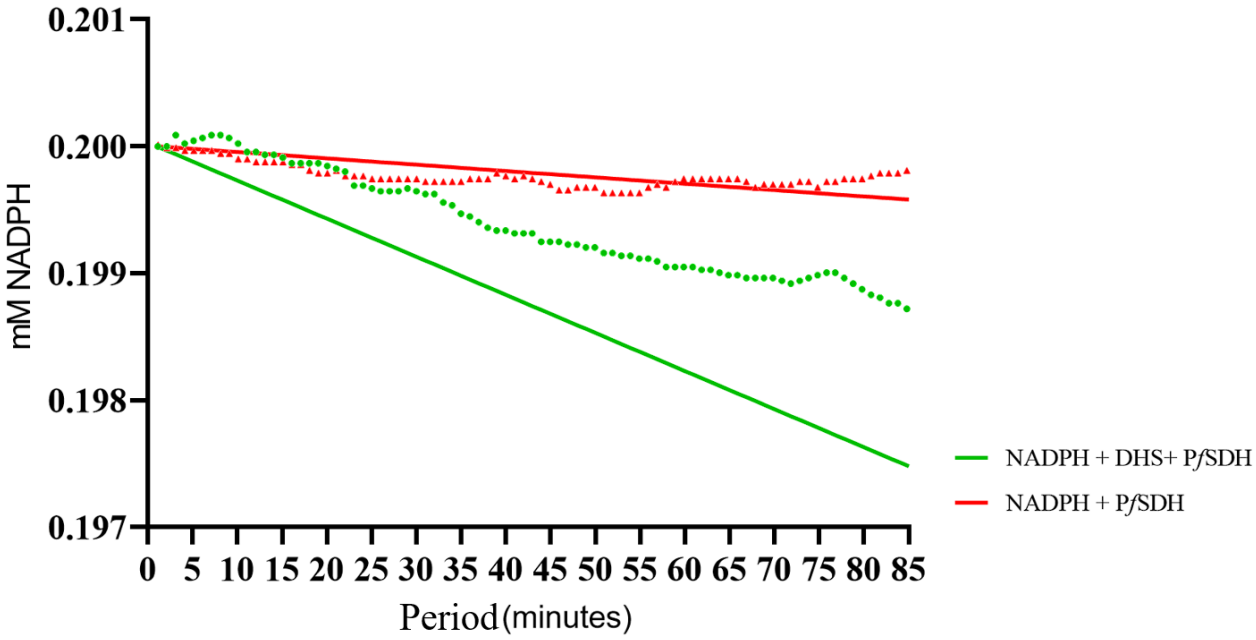

Figure 7. P*f*SDH enzymatic activity applying linear reaction. Reaction measured by the reduction of NADPH in linear interaction mode with DHS mediated by P*f*SDH catalysis. Enzyme activity measured via absorbance at 340 nm during the elapsed time from the beginning of reaction. Green: catalysis of DHS by P*f*SDH with NADPH as a cofactor. Red: NADPH cofactor and P*f*SDH enzyme as the control.

negligible or non-existent (Zhao et al. 2018). The induction period is a relevant factor to be taken into consideration, since the OD_{600} for IPTG 0.1 mM remained approximately the same between 48 and 72 hours (4.408 and 4.404, respectively); it is preferable that the shorter period is used so that work time and process-related costs are reduced.

Comparing the results from the SDS-PAGE (Figure 4a, b and c) with the bacterial growth curve (Figure 3), it was decided to select only the 24- and 48-hour samples for the step of lysis, both with 0.1 mM IPTG. In cell lysis (Figure 4d), the application of the lysis buffer was effective in destroying *E. coli* BL21(DE3) cells and releasing P*f*SDH in a predominantly soluble form (S). Thus, the best induction time after lysis was 48 hours, as it presented a higher OD_{600} in the bacterial growth curve (Figure 3). Therefore, we consider that the ideal parameters for effective cell growth and induction of P*f*SDH expression in *E. coli* BL21(DE3) are 0.1 mM IPTG after OD_{600} = 0.6 for 48 hours at 37 °C and shaking at 200 rpm.

A single peak observed in the absorbance of 280 nm after the beginning of imidazole gradient (Figure 6a) is a standard characteristic when purifying proteins with the polyhistidine tag using IMAC, which, due to the high degree of affinity and interaction specificity, is generally applied in a sufficiently efficient single step (Spriestersbach et al. 2015). Final concentration of imidazole at 250 mM was necessary to elute P*f*SDH because it is coupled to a tag with six histidine, which interacts with more active sites during the binding phase to the Ni-NTA agarose resin than a four-histidine tag (which is more often used), requiring a higher concentration of imidazole for the effective elution of the recombinant protein (Riguero et al. 2020).

This higher band present in the eluate (Figure 6) may be an endogenous *E. coli* protein, given that copurification of these proteins is common, especially when the expression

level of the recombinant polyhistidine-tagged protein is low, as is the case of P*f*SDH (Structural Genomics Consortium et al. 2008). These non-specific copurified molecules are proteins with multiple histidine or molecular chaperones, which bind to the resin or recombinant protein during the purification process, and which are produced endogenously by *E. coli* in response to the stress caused by heterologous protein expression (Bolanos-Garcia & Davies 2006). In this way, efforts to increase sample purity were applied using a two-step IMAC purification (Figure 6c) even though these successive purifications can have the undesired effect of excessively decreasing protein concentration (Fernandez-Soto et al. 2020; Fonseca et al. 2006).

Regarding physiological activity analysis of P*f*SDH, given that the NADP+ by-product absorbs UV light at a wavelength of 260 nm, its emergence in the solution after reaction does not interfere with the monitored absorbance (Fruscione et al. 2008). The reaction control consisted of analyzing the existence of an interaction between 0.2 mM NADPH and 855 µg/mL P*f*SDH excluding DHS. If NADPH oxidation occurs only via the catalysis of P*f*SDH, the curve would have the same slope rate as in the presence of DHS. However, there is a slight slope showing a little oxidation caused by another component resulting from the whole process.

A slight downward trend can be observed in the absence of the substrate (NADPH + P*f*SDH), leading to the assumption that there was a small consumption of NADPH. This consumption may be linked to the reaction of NADPH by the Fre-MsrQ complex, an analogue of NADPH oxidase (NOX) present in *E. coli*, while catalyzing atmospheric oxygen (O_2) (Juillan-Binard et al. 2017), and not being expressive in the P*f*SDH reaction observed. This complex might be present due to copurification of endogenous proteins (Fonseca et al. 2006). The catalytic reaction of P*f*SDH could be observed as effectively occurring throughout the experiment, with a noticeable reduction in absorbance at 340 nm through monitoring of NADPH, thus confirming the maintenance of recombinant P*f*SDH catalytic activity when applying the expression protocol described in the present study.

Since P*f*SDH physiological catalytic activity is specific to the reaction between DHS and NADPH, and this reaction could be observed through NADPH oxidation under the circumstances described above, we suggest that its nucleotide sequence (XM_001348562) status as being putative is no longer accurate.

CONCLUSIONS

This study showed the effective recombinant expression in an *E. coli* BL21(DE3) system of *Plasmodium falciparum* shikimate dehydrogenase (P*f*SDH) inserted in a pET28a vector. Different induction conditions were explored during the expression phase; however, it was possible to conclude that, during the induction phase, applying IPTG 0.1 mM for 48 hours and at 37 °C achieves an OD_{600} of 4.408, which was the highest among the parameters sampled, thus enabling one to start this phase with as many cells as possible. During the solubilization phase, it was possible to extract predominantly soluble recombinant P*f*SDH, and the application of immobilized nickel ions affinity chromatography was effective in separating most of the soluble content after the lysis process. We also showed that, despite a low yield and not reaching an ideal condition of purity, P*f*SDH was shown to be enzymatically active, thus validating the protocol developed for its expression. Finally, we formulated the first protocol for the recombinant expression of a shikimate dehydrogenase (SDH) for the genus

Plasmodium sp., specifically for *P. falciparum*, and we are confident that the steps described in this study can help further studies to obtain this enzyme for other types of analysis, such as applying it as a molecular target for screening of its enzymatic inhibition activity.

Acknowledgments

The present research was funded by Fundação de Amparo ao Desenvolvimento das Ações Científicas e Tecnológicas e à Pesquisa de Rondônia (FAPERO) – Brazil (Proc. No. 0012427590201812.052/2018) and by Instituto Nacional de Epidemiologia na Amazônia Ocidental (INCT-EPIAMO) – Brazil (Proc. No. 465657/2014-1). This study was financed in part by the Coordenação de Aperfeiçoamento de Pessoal de Nível Superior – Brasil (CAPES) – Finance Code 001, which provided a Doctorate Scholarship to B. Morales (Proc. No. 88887.633028/2021-00).

REFERENCES

ALTSCHUL SF, GISH W, MILLER W, MYERS EW & LIPMAN DJ. 1990. Basic local alignment search tool. J Mol Biol 215: 403-410. https://doi.org/10.1016/s0022-2836(05)80360-2.

BOLANOS-GARCIA VM & DAVIES OR. 2006. Structural analysis and classification of native proteins from *E. coli* commonly co-purified by immobilized metal affinity chromatography. Biochim Biophys Acta 1760: 1304-1313. https://doi.org/10.1016/j.bbagen.2006.03.027.

BOUGARD C, ALBRECHT L, KAYANO ACAV, SUNNERHAGEN P & COSTA FTM. 2018. *Plasmodium vivax* Biology: Insights Provided by Genomics, Transcriptomics and Proteomics. Front Cell Infect Microbiol 34: 1-22. https://doi.org/10.3389/fcimb.2018.00034.

BOZDECH Z, LLINÁS M, PULLIAM BL, WONG ED, ZHU J & DERISI JL. 2003. The Transcriptome of the Intraerythrocytic Developmental Cycle of *Plasmodium falciparum*. PLOS Biol 1: 85-100. https://doi.org/10.1371/journal.pbio.0000005.

CENTERS FOR DISEASE CONTROL AND PRESERVATION. 2019. Malaria, Disease. https://www.cdc.gov/malaria/about/disease.html.

DÍAZ-QUIROZ DC, CARDONA-FÉLIX CS, VIVEROS-CEBALLOS JL, REYES-GONZÁLEZ MA, BOLÍVAR F, ORDOÑEZ M & ESCALANTE A. 2018. Synthesis, biological activity and molecular modelling studies of shikimic acid derivatives as inhibitors of the shikimate dehydrogenase enzyme of *Escherichia coli*. J Enzyme Inhib Med Chem 33: 397-404. https://doi.org/10.1080/14756366.2017.1422125.

DONDORP AM, PONGPONRATN E & WHITE NJ. 2004. Reduced microcirculatory flow in severe falciparum malaria: pathophysiology and electron-microscopic pathology. Acta Trop 89: 309-317. https://doi.org/10.1016/j.actatropica.2003.10.004.

EINSFELDT K, SEVERO JÚNIOR JB, ARGONDIZZO APC, MEDEIROS MA, ALVES TAM, ALMEIDA RV & LARENTIS AL. 2011. Cloning and expression of protease ClpP from *Streptococcus pneumoniae* in *Escherichia coli*: study of the influence of kanamycin and IPTG concentration on cell growth, recombinant protein production and plasmid stability. Vaccine 29: 7136-7143. https://doi.org/10.1016/j.vaccine.2011.05.073.

FAIRHURST RM & DONDORP AM. 2016. Artemisinin-resistant *Plasmodium falciparum* malaria. Microbiol Spectr 4: 1-25. https://journals.asm.org/doi/10.1128/microbiolspec.EI10-0013-2016.

FERNANDEZ-SOTO P, CAVET JS & TABERNERO L. 2020. Expression and purification of soluble recombinant SapM from *Mycobacterium tuberculosis*. Protein Expr Purif 174: 1-8. https://doi.org/10.1016/j.pep.2020.105663.

FERREIRA LG, OLIVA G & ANDRICOPULO AD. 2018. From Medicinal Chemistry to Human Health: Current Approaches to Drug Discovery for Cancer and Neglected Tropical Diseases. An Acad Bras Cienc 90: 645-661. https://doi.org/10.1590/0001-3765201820170505.

FONSECA IO, MAGALHÃES MLB, OLIVEIRA JS, SILVA RG, MENDES MA, PALMA MS, SANTOS DS & BASSO LA. 2006. Functional shikimate dehydrogenase from *Mycobacterium tuberculosis* H37Rv: purification and characterization. Protein Expr Purif 46: 429-437. https://doi.org/10.1016/j.pep.2005.10.004.

FRUSCIONE F, STURLA L, DUNCAN G, ETTEN JLV, VALBUZZI P, FLORA A, ZANNI E & TONETTI M. 2008. Differential role of NADP+ and NADPH in the activity and structure of GDP-D-mannose 4,6-dehydratase from two chlorella viruses. J Biol Chem 283: 184-193. https://doi.org/10.1074/jbc.m706614200.

GARDNER MJ ET AL. 2002. Genome sequence of the human malaria parasite *Plasmodium falciparum*. Nature 419: 498-511. https://doi.org/10.1038/nature01097.

GASTEIGER E, HOOGLAND C, GATTIKER A, DUVAUD S, WILKINS MR, APPEL RD & BAIROCH A. 2005. Protein Identification and Analysis Tools on the ExPASy Server. In: Walker JM (Ed), The Proteomics Protocols Handbook, Totowa: Humana Press, p. 571-607.

HIRANO S. 2012. Western blot analysis. Methods Mol Biol 926: 87-97. https://doi.org/10.1007/978-1-62703-002-1_6.

JUILLAN-BINARD C, PICCIOCCHI A, ANDRIEU JP, DUPUY J, PETIT-HARTLEIN I, CAUX-THANG C, VIVÈS C, NIVIÈRE V & FIESCHI F. 2017. A Two-component NADPH Oxidase (NOX)-like System in Bacteria Is Involved in the Electron Transfer Chain to the Methionine Sulfoxide Reductase MsrP. J Biol Chem 292: 2485-2494. https://doi.org/10.1074%2Fjbc.M116.752014.

KUMAR S, BHARDWAJ TR, PRASAD DN & SINGH RK. 2018. Drug targets for resistant malaria: Historic to future perspectives. Biomed Pharmacother 104: 8-27. https://doi.org/10.1016/j.biopha.2018.05.009.

LAEMMLI UK. 1970. Cleavage of Structural Proteins during the Assembly of the Head of Bacteriophage T4. Nature 227: 680-685. https://doi.org/10.1038/227680a0.

LOUGHRAN ST, BREE RT & WALLS D. 2017. Purification of Polyhistidine-Tagged Proteins. Methods Mol Biol 1485: 275-303. https://doi.org/10.1007/978-1-4939-6412-3_14.

MARÍ YM, ESPINOSA AE, UBIETA R, BATISTA OF & FERNÁNDEZ ML. 1999. Effect of the selection marker on the viability and plasmid stability of two human proteins with neurotrophic action expressed in *Escherichia coli*. Biochem Biophys Res Commun 258: 29-31. https://doi.org/10.1006/bbrc.1999.0568.

MCCONKEY GA. 1999. Targeting the Shikimate Pathway in the Malaria Parasite *Plasmodium falciparum*. Antimicrob Agents Chemother 43: 175-177. https://doi.org/10.1128/aac.43.1.175.

NATIONAL CENTER FOR BIOTECHNOLOGY INFORMATION. 2019. GenBank, *Plasmodium sp*. gorila clade G2 conserved Plasmodium protein, unknown function (PADL01_1444700), partial mRNA. https://www.ncbi.nlm.nih.gov/nuccore/XM_028684730.

PETTY KJ. 2001. Metal-Chelate Affinity Chromatography. Curr Protoc Mol Biol 10: 10-24. https://doi.org/10.1002/0471142727.mb1011bs36.

RIGUERO V, CLIFFORD R, DAWLEY M, DICKSON M, GASTFRIEND B, THOMPSON C, WANG S & O'CONNOR E. 2020. Immobilized metal affinity chromatography optimization for poly-histidine tagged proteins. J Chromatogr A 461505: 1-19. https://doi.org/10.1016/j.chroma.2020.461505.

SAMBROOK J & RUSSELL DW. 2001. Molecular cloning: a laboratory manual, 3rd ed., New York: Cold Spring Harbor Laboratory Press, 2100 p.

SCHNEIDER CA, RASBAND WS & ELICEIRI KW. 2012. NIH Image to ImageJ: 25 years of image analysis. Nature Methods 9: 671-675. https://doi.org/10.1038/nmeth.2089.

SHILLING PJ, MIRZADEH K, CUMMING AJ, WIDESHEIM M, KÖCK Z & DALEY DO. 2020. Improved designs for pET expression plasmids increase protein production yield in *Escherichia coli*. Commun Biol 3: 1-8. https://doi.org/10.1038/s42003-020-0939-8.

SIEVERS F ET AL. 2011. Fast, scalable generation of high-quality protein multiple sequence alignments using Clustal Omega. Mol Syst Biol 539: 1-6. https://doi.org/10.1038/msb.2011.75.

SPRIESTERSBACH A, KUBICEK J, SCHÄFER F, BLOCK H & MAERTENS B. 2015. Purification of His-Tagged Proteins. Methods Enzymol 559: 1-15. https://doi.org/10.1016/bs.mie.2014.11.003.

STRUCTURAL GENOMICS CONSORTIUM ET AL. 2008. Protein production and purification. Nature Methods 5: 135-146. https://doi.org/10.1038/nmeth.f.202.

SUNDARARAMAN SA ET AL. 2016. Genomes of cryptic chimpanzee Plasmodium species reveal key evolutionary events leading to human malaria. Nat Commun 7: 11078. https://doi.org/10.1038/ncomms11078.

SUTTON KA, BREEN J, RUSSO TA, SCHULTZ LW & UMLAND TC. 2016. Crystal structure of 5-enolpyruvylshikimate-3-phosphate (EPSP) synthase from the ESKAPE pathogen *Acinetobacter baumannii*. Acta Crystallogr F Struct Biol Commun 7: 179-187. https://doi.org/10.1107/s2053230x16001114.

VESKOUKIS AS, MARGARITELIS NV, KYPAROS A, PASCHALIS V & NIKOLAIDIS MG. 2018. Spectrophotometric assays for measuring redox biomarkers in blood and tissues: the NADPH network. Redox Rep 23: 47-56. https://doi.org/10.1080/13510002.2017.1392695.

WATERHOUSE AM, PROCTER JB, MARTIN DMA, CLAMP M & BARTON GJ. 2009. Jalview Version 2-a multiple sequence alignment editor and analysis workbench. Bioinformatics 25: 1189-1191. https://doi.org/10.1093/bioinformatics/btp033.

WORLD HEALTH ORGANIZATION. 2022. World malaria report 2022. https://www.who.int/publications/i/item/9789240064898.

XU J, LI W, WU J, ZHANG Y, ZHU Z, LIU J & HU Z. 2006. Stability of plasmid and expression of a recombinant gonadotropin-releasing hormone (GnRH) vaccine in *Escherichia coli*. Appl Microbiol Biotechnol 73: 780-788. https://doi.org/10.1007/s00253-006-0547-7.

ZHAO M, TAO X, WANG F, REN Y & WEI D. 2018. Establishment of a low-dosage-IPTG inducible expression system construction method in *Escherichia coli*. J Basic Microbiol 58: 806-810. https://doi.org/10.1002/jobm.201800160.

How to cite
MORALES BGDV, EVARISTO JAM, OLIVEIRA GAR, GARAY AFG, DIAZ JJAR, ARRUDA A, PEREIRA SS & ZANCHI FB. 2024. Expression and purification of active shikimate dehydrogenase from *Plasmodium falciparum*. An Acad Bras Cienc 96: e20230382. DOI 10.1590/0001-3765202420230382.

Manuscript received on April 2, 2023; accepted for publication on October 2, 2023

BRUNO G. DALLA VECCHIA MORALES[1,2,3]
https://orcid.org/0000-0003-3678-5586

JOSEPH ALBERT M. EVARISTO[1]
https://orcid.org/0000-0001-5401-1758

GEORGE A.R. DE OLIVEIRA[1,4]
https://orcid.org/0000-0002-9210-9649

ANA FIDELINA G. GARAY[5]
https://orcid.org/0000-0003-3737-7015

JORGE JAVIER A.R. DIAZ[5]
https://orcid.org/0000-0003-3189-0037

ANDRELISSE ARRUDA[6,7]
https://orcid.org/0000-0002-3685-2630

SORAYA S. PEREIRA[2,6]
https://orcid.org/0000-0003-2116-7670

FERNANDO B. ZANCHI[1,2,4]
https://orcid.org/0000-0003-3386-0069

[1]Oswaldo Cruz Foundation Rondônia (FIOCRUZ/RO), Laboratory of Bioinformatics and Medicinal Chemistry, BR 364, km 9,5, Centro, 76801-059 Porto Velho, RO, Brazil

[2]Federal University of Rondonia (UNIR), BR 364, km 9,5, Centro, 76801-059 Porto Velho, RO, Brazil

[3]São Lucas University Center (UniSL), Alexandre Guimarães Street, 1927, Areal, 76804-373 Porto Velho, RO, Brazil

[4]Oswaldo Cruz Institute (IOC), Brasil Avenue 4365, Manguinhos, 21040-900 Rio de Janeiro, RJ, Brazil

[5]Centro para el Desarrollo de la Investigación Científica (CEDIC), P975+F58, Manduvira, Asuncion, Paraguay

[6]Oswaldo Cruz Foundation Rondônia (FIOCRUZ/RO), Laboratory of Antibodies Engineering, Beira Street, 7671, Lagoa, 76812-245 Porto Velho, RO, Brazil

[7]Oswaldo Cruz Foundation Brasília (FIOCRUZ BRASÍLIA), L3 North Avenue, Gleba A, 70904-130 Brasília, DF, Brazil

Correspondence to: **Bruno Gildo Dalla Vecchia Morales**
E-mail: brunogdvm@gmail.com

Author contributions

Author contributions under CRediT terms. B. G. D. V. Morales: Data Curation, Formal analysis, Investigation, Methodology, Project administration, Validation, Visualization, Writing - Original Draft, Writing - Review & Editing. J. A. M. Evaristo: Investigation, Methodology, Validation. G. A. R. Oliveira: Investigation, Methodology, Validation. A. F. G. Garay: Investigation, Validation. J. J. A. R. Diaz: Investigation, Validation. A. Arruda: Investigation¸ Methodology, Validation. S. S. Pereira: Investigation, Methodology, Resources, Supervision, Validation. F. B. Zanchi: Conceptualization, Data Curation, Formal analysis, Funding acquisition, Investigation, Methodology, Project administration, Resources, Supervision and Writing - Review & Editing.